



Molecular Crystals and Liquid Crystals Science and Technology. Section A. Molecular Crystals and Liquid Crystals

Publication details, including instructions for authors and subscription information:

<http://www.tandfonline.com/loi/gmcl19>

Influence of the Distribution General Shape of n-Alkane Molar Concentrations on the Structural State of Multi-Alkane Mixtures

V. Chevallier^a, A. J. Briard^a, D. Petitjean^a, N. Hubert^a, M. Bouroukba^a & M. Dirand^a

^a Laboratoire de Thermodynamique des Séparations
Ecole Nationale Supérieure des Industries Chimiques
Institut National Polytechnique de Lorraine 1, rue
Grandville - BP 451, 54001, NANCY CEDEX, FRANCE

Version of record first published: 24 Sep 2006

To cite this article: V. Chevallier, A. J. Briard, D. Petitjean, N. Hubert, M. Bouroukba & M. Dirand (2000): Influence of the Distribution General Shape of n-Alkane Molar Concentrations on the Structural State of Multi-Alkane Mixtures, Molecular Crystals and Liquid Crystals Science and Technology. Section A. Molecular Crystals and Liquid Crystals, 350:1, 273-291

To link to this article: <http://dx.doi.org/10.1080/10587250008025250>

Full terms and conditions of use: <http://www.tandfonline.com/page/terms-and-conditions>

This article may be used for research, teaching, and private study purposes. Any substantial or systematic reproduction, redistribution, reselling, loan, sub-licensing, systematic supply, or distribution in any form to anyone is expressly forbidden.

The publisher does not give any warranty express or implied or make any representation that the contents will be complete or accurate or up to date. The accuracy of any instructions, formulae, and drug doses should be independently verified with primary sources. The publisher shall not be liable for any loss, actions, claims, proceedings, demand, or costs or damages whatsoever or howsoever caused arising directly or indirectly in connection with or arising out of the use of this material.

Influence of the Distribution General Shape of n-Alkane Molar Concentrations on the Structural State of Multi-Alkane Mixtures

V. CHEVALLIER, A.J. BRIARD, D. PETITJEAN, N. HUBERT,
M. BOUROUKBA and M. DIRAND*

*Laboratoire de Thermodynamique des Séparations Ecole Nationale Supérieure
des Industries Chimiques Institut National Polytechnique de Lorraine 1,
rue Grandville – BP 451 – 54001 NANCY CEDEX FRANCE*

(Received March 31, 2000)

X-ray diffraction analyses were carried out on four commercial multi-alkane samples and their fifty-fifty weight mixtures which present molar concentration distributions of the "normal logarithmic" type: all these systems form a single solid phase which is isostructural to the β' ordered intermediate solid solution of n-alkane binary molecular alloys: they are the n-alkanes with carbon atom numbers, n, close to the mean composition in carbon atoms of the mixtures which are in the majority and which impose a single molecule layer thickness. Structural and differential thermal analyses highlighted in the course of cooling from liquid state the successive appearance of three solid solutions in a synthetic mixture whose the molar concentration distribution (from C_{18} to C_{36}) has a shape of the "decreasing exponential" type as observed in petroleum cuts: the smaller chains, which here are in the majority, do not succeed in making the longer chains bend, too numerous, to form a single solid solution.

Keywords: n-alkanes; multicomponent; structures

1. INTRODUCTION

Petroleum fluids, such as paraffinic cuts, contain heavy hydrocarbons which can crystallize during the extraction, the transportation through the pipelines and the refining process. The solid deposits, which block pipelines and filters, are a

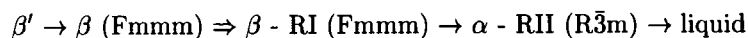
* corresponding author: Tel: 33.3.83.17.50.07, Fax: 33.3.83.17.50.76, E-mail address: mdirand@ensic.u-nancy.fr

major issue in the deterioration of the equipment of the petroleum industry. In order to find a remedy for these risks, it is necessary to be able to represent and predict the thermodynamic behavior of phases of crude oils, particularly those of the solid deposits. Up to now industrial and commercial multi-alkane samples, which have been studied in literature [1–4], show a continuous distribution of consecutive n-alkane (hereafter denoted by C_n) molar concentrations of the “normal logarithmic” type. However in the petroleum fluids, the molar concentrations of C_n are regularly decreasing as a function of n carbon atoms. The aim of this study is to determine and to compare the structural and thermodynamic state of multi- C_n commercial mixtures with “normal logarithmic” type distributions and a synthetic mixture whose C_n molar concentrations show a distribution of the “decreasing exponential” type.

2. SOME LITERATURE RESULTS

With regard to commercial multi- C_n solid samples, which mainly consist of many consecutive C_n (from 20 up to 33) with chain lengths between 20 and 52 carbon atoms whose molar concentrations present a distribution of “normal logarithmic” type, the structural observations, that were carried out by X-ray diffraction by DIRAND *et al.* [3] and by CHEVALLIER *et al.* [4], show that these multi- C_n mixtures form a single solid solution, whose orthorhombic structure is isostructural to the β' ordered intermediate phase of binary and ternary C_n alloys [5–7]: a single periodicity of the molecule layer stacking along the long crystallographic c-axis is observed; it corresponds to the chain length of a hypothetical orthorhombic pure C_n with a number of carbon atoms equal to the mean composition of carbon atoms of multi- C_n mixtures with an excess value close to one carbon atom in relation to the results of chromatographic analyses. These experimental results [3, 4] are in agreement with those of RETIEF and Le ROUX [1] and CRAIG *et al.* [2] who respectively studied paraffinic FISCHER-TROPSCH waxes and solid deposits of real diesel wax systems.

With increasing temperatures the β' binary, ternary or multi- C_n intermediate solid solution undergoes the following solid-solid transitions, identical to those of the orthorhombic pure C_{23} [5,7,8] (Fig. 1):



where \rightarrow denotes first-order transitions, and \Rightarrow higher-order transitions.

i) the occurrence of the β (Fmmm) disordered phase is accompanied by a splitting of the (0 2 0) diffraction peak (Fig. 1c-d-e) and the disappearance of Bragg-diffractions whose (h k ℓ) indices do not have a same parity; then the new

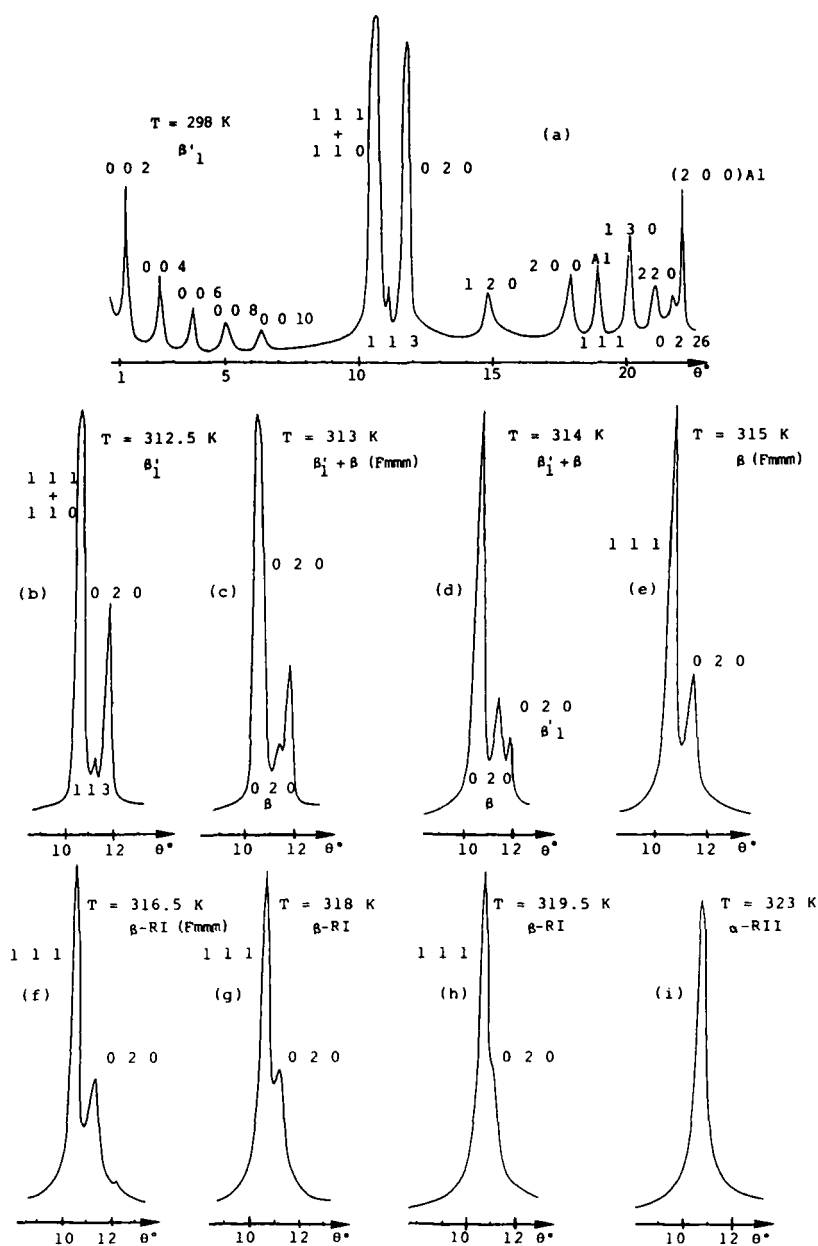


FIGURE 1 Structural evolutions of the β' intermediate solid solution observed by X-ray diffraction (θ° - λ Cu K_α) when the temperature increases

(0 2 0) line moves toward the (1 1 1) diffraction peak (Fig. 1f-g-h): this structural behavior characterizes the RI Rotator state of this β (Fmmm) phase as highlighted by MULLER [9], UNGAR [10], DOUCET *et al.* [11] and UNGAR and MASIC [12] for the pure C_{23} and corresponds to a solid-solid transition of a order higher than one [10,12].

ii) when the two (0 2 0) and (1 1 1) diffraction lines coincide (Fig. 1i), the symmetry of the unit cell base (a,b) becomes hexagonal and the mixtures undergo a further weak first-order transition into the α rhombohedral phase in RII Rotator state whose space group $R\bar{3}m$ has been determined by UNGAR [10] and UNGAR and MASIC [12].

Concerning the multiparaffin synthetic mixtures whose C_n molar concentrations show a “decreasing exponential” type distribution, studies were carried out by chromatographic analyses of phase fractions separated at liquid-solid equilibrium in the course of their crystallization in C_{10} [13–15]: the variation of the composition of the solid and liquid phases were characterized as a function of the temperature below the crystallization onset temperature.

3. EXPERIMENTAL

The paraffin mixtures, that show distributions of C_n molar concentrations of the “normal logarithmic” type (Fig. 2), were purchased from PROLABO: they are called paraffin 52–54°C, 54–56°C, 58–60°C, 60–62°C in its commercial catalogue and respectively denoted sample No 1, No 2, No 3 and No 4. The C_n concentrations of these paraffin mixtures were determined by gas chromatography and spectrometry analyses (Table I and Fig. 2). Mixtures, denoted (Para i,j), were made up of samples No i and j with fifty-fifty weight percent (i and j different and varying from 1 to 4).

TABLE I Molar percent concentrations of C_n in multi-paraffinic samples No 1 to 4 and in Para i,j mixtures of No i and j samples: the concentration distributions present the « normal logarithmic » type

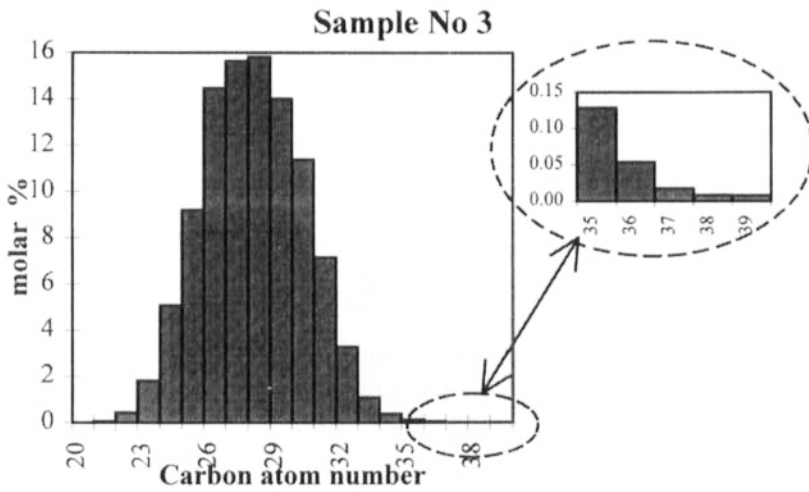
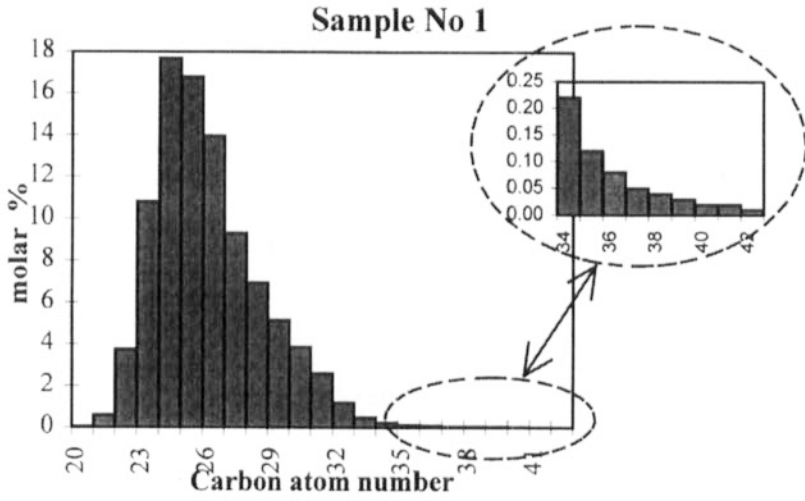
	No 1	No 2	No 3	No 4	Para 1,2	Para 1,3	Para 1,4	Para 2,3	Para 2,4	Para 3,4
C ₂₀	0.07	0.05	0.02	0.04	0.06	0.04	0.06	0.03	0.04	0.03
C ₂₁	0.77	0.45	0.06	0.18	0.62	0.44	0.52	0.26	0.33	0.12
C ₂₂	4.63	2.89	0.44	0.68	3.81	2.71	2.99	1.69	1.91	0.55
C ₂₃	12.82	8.00	1.81	2.08	10.54	7.76	8.35	4.99	5.38	1.93
C ₂₄	20.09	13.10	5.08	4.25	16.79	13.20	13.50	9.20	9.19	4.70
C ₂₅	18.32	14.35	9.19	6.59	16.44	14.13	13.44	11.84	10.91	8.01

	No 1	No 2	No 3	No 4	Para 1,2	Para 1,3	Para 1,4	Para 2,3	Para 2,4	Para 3,4
C ₂₆	14.64	15.46	14.46	8.48	15.03	14.56	12.07	14.97	12.37	11.73
C ₂₇	9.40	13.26	15.63	10.62	11.22	12.26	9.91	14.41	12.09	13.34
C ₂₈	6.76	11.44	15.81	11.76	8.97	10.91	8.84	13.56	11.58	13.96
C ₂₉	4.85	8.85	14.00	11.72	6.74	9.05	7.71	11.36	10.12	12.96
C ₃₀	3.51	6.24	11.37	10.38	4.80	7.13	6.37	8.74	8.07	10.92
C ₃₁	2.28	3.45	7.14	8.81	2.83	4.52	5.00	5.24	5.82	7.90
C ₃₂	1.02	1.56	3.28	6.70	1.27	2.06	3.38	2.40	3.84	4.84
C ₃₃	0.39	0.56	1.10	5.07	0.47	0.72	2.34	0.82	2.56	2.91
C ₃₄	0.18	0.21	0.38	3.57	0.19	0.27	1.59	0.29	1.70	1.84
C ₃₅	0.09	0.08	0.13	2.59	0.09	0.11	1.13	0.10	1.19	1.25
C ₃₆	0.06	0.03	0.05	1.83	0.05	0.06	0.80	0.04	0.83	0.86
C ₃₇	0.04	0.02	0.02	1.42	0.03	0.03	0.61	0.02	0.64	0.66
C ₃₈	0.03	0.01	0.01	1.04	0.02	0.02	0.45	0.01	0.46	0.48
C ₃₉	0.02	0.01	0.01	0.64	0.01	0.02	0.28	0.01	0.29	0.30
C ₄₀	0.01	0.01	0.00	0.49	0.01	0.01	0.21	0.00	0.22	0.22
C ₄₁	0.01	–	–	0.32	0.01	0.01	0.14	0.01	0.14	0.15
C ₄₂	0.01	–	–	0.25	0.00	0.00	0.11	0.01	0.11	0.11
C ₄₃	–	–	–	0.16	–	–	0.07	–	0.07	0.07
C ₄₄	–	–	–	0.11	–	–	0.05	–	0.05	0.05
C ₄₅	–	–	–	0.07	–	–	0.03	–	0.03	0.03
C ₄₆	–	–	–	0.06	–	–	0.02	–	0.03	0.03
C ₄₇	–	–	–	0.03	–	–	0.01	–	0.01	0.01
C ₄₈	–	–	–	0.02	–	–	0.01	–	0.01	0.01
C ₄₉	–	–	–	0.02	–	–	0.01	–	0.01	0.01
C ₅₀	–	–	–	0.02	–	–	0.01	–	0.01	0.01
C ₅₁	–	–	–	0.01	–	–	0.00	–	0.00	0.00
C ₅₂	–	–	–	0.01	–	–	0.00	–	0.00	0.00
\bar{n}	25.6	26.4	27.8	29.4	26.0	26.6	27.4	27.1	27.7	28.5

The mean number of carbon atoms, \bar{n} , was calculated from the x_n molar fractions of C_n, that were determined by gas chromatography analyses, using the following relationship:

$$\bar{n} = \sum_{n_{\min}}^{n_{\max}} n \cdot x_n$$

where x_n is the molar fraction of each C_n, n_{\max} and n_{\min} the carbon atom numbers of the longer and smaller C_n chains respectively in the multi-C_n mixture.



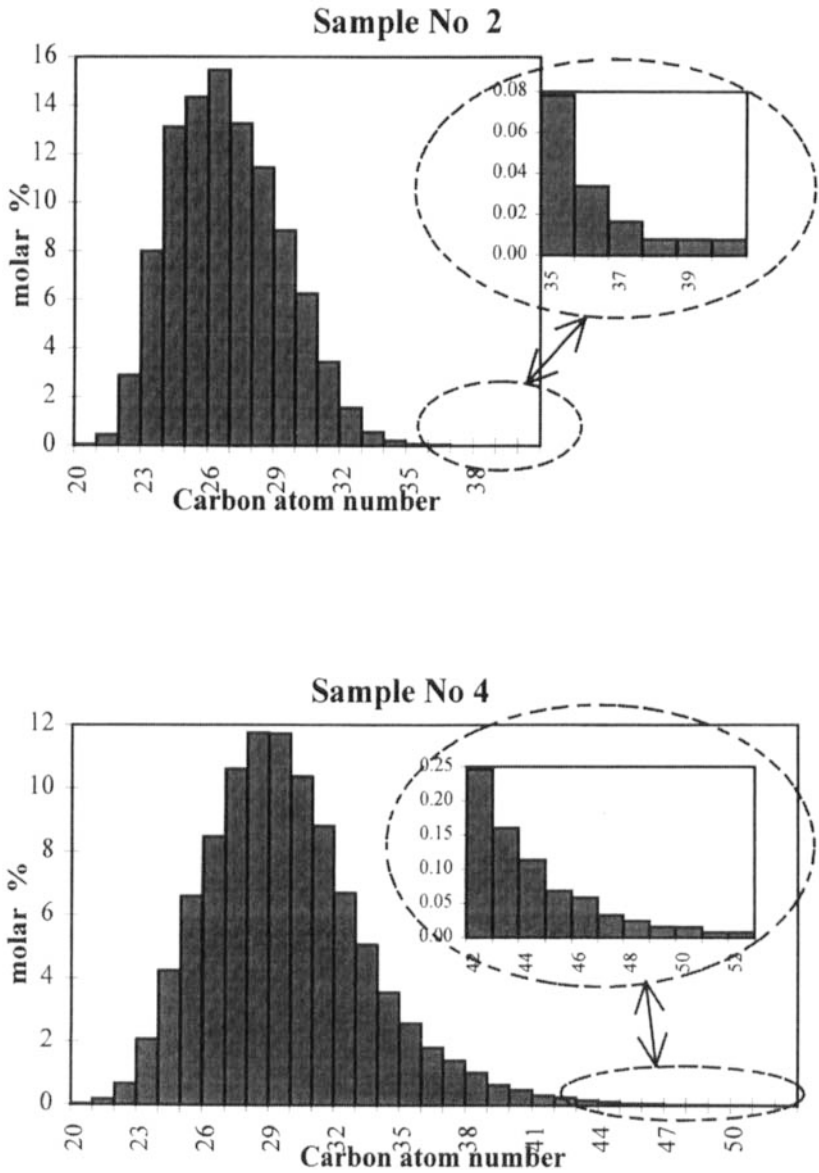


FIGURE 2 C_n molar percent concentration distributions of the “normal logarithmic” type in commercial samples No 1, 2, 3, 4

The synthetic mixture with a C_n molar concentration distribution of the "decreasing exponential" type (Fig. 3) was prepared by weighing together the solid pure C_n , melting and thoroughly mixing. Then the homogeneous liquid solution was allowed to cool at the ambient temperature. The pure C_n were purchased from Aldrich Chemical Company: their purity grade is 99 mol % as determined by gas chromatography. The sample was composed of the full series of C_n within which the x_n molar fraction of C_n is regularly decreasing from C_{18} to C_{36} (Fig. 3) according to the following recurrence relationship:

$$x_{n+1} = \alpha x_n$$

where the coefficient ($\alpha = 0.858$) was fixed at in such a way as to match the average compositions observed in waxy crude oils; the \bar{n} average number of carbon atoms of the synthetic mixture is equal to 23. The synthetic mixture (C_{18} from C_{36}) is denoted sample No 5.

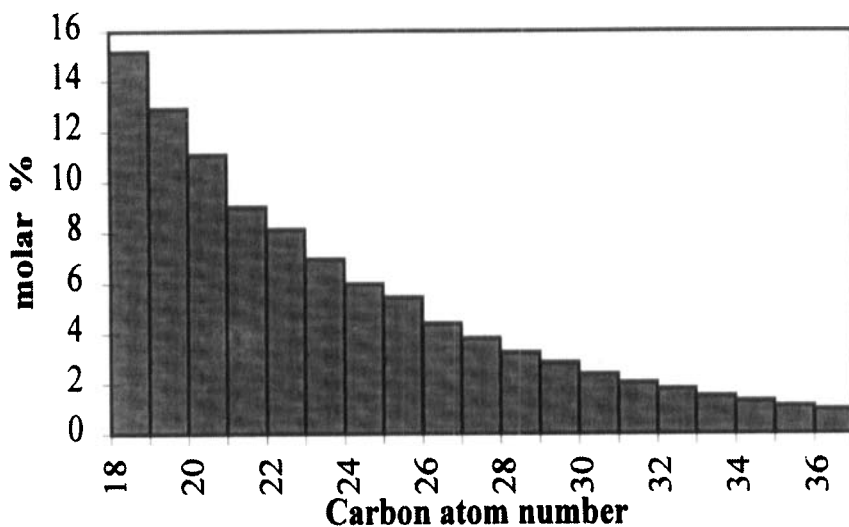


FIGURE 3 C_n molar percent concentration distribution of the "decreasing exponential" type in sample No 5 (C_{18} - C_{36}): $x_{n+1} = \alpha \cdot x_n$ with $\alpha = 0.858$

X-ray diffraction experiments were carried out on the samples using $\lambda K\alpha$ copper or cobalt radiations. The X-ray patterns were obtained with CGR diffractometers (Theta 60) and the X-ray diffraction analyses were performed at different temperatures with the help of a heated sample holder; heating or cooling of the sample holder was based on the Peltier effect: the precision of the sample tem-

perature was within ± 0.5 K of the set point. In order to study the structural behavior from the solid state up to liquid state and vice versa, the $\theta/2\theta$ goniometer is fixed on a vertical table so that the sample holder is initially in a horizontal position. A motor makes the table turn at the same angular rate as the goniometer, but the other way round, so that the sample holder is kept in horizontal position [16]. The samples were heated or cooled with a rate of 1 K.mn^{-1} between two successive isothermal levels: the length of each isothermal level was equal to one hour.

The focused monochromatic beam was obtained with a filament intensity of 10 mA at 48 kV and the line positions were measured with an accuracy of 0.05° for each value of Bragg angles: the calibration was done with pure aluminium as standard, of which the sample holder was made.

The preparation of powder samples has already been described [5,6]. However, in order to increase the intensity of the $(0\ 0\ \ell)$ diffraction lines by preferential crystallographic orientations, samples were prepared by melting and low cooling of waxes on a water surface. This mode of sample preparation do not change the structural state of multi- C_n mixtures; moreover the structural state of multi- C_n mixtures, which show "normal logarithmic" type distributions, is identical after an ageing of three years.

RESULTS

Mixtures with C_n molar concentration distributions of the "normal logarithmic" type

A single family of $(0\ 0\ \ell)$ diffraction peaks appears on all the diffractograms-X, carried out on samples No i (i varying from 1 to 4) and Para i,j (i and j different and varying from 1 to 4) at 287.15 K: in order to illustrate this phenomenon, Fig. 4 compares the X-ray diffraction scattering patterns, respectively obtained from a mixture of the powders of pure C_n ($28 \leq n \leq 36$) that were not melted together (Fig. 4a) and multi- C_n sample No 1 (Fig. 4b).

The many series of $(0\ 0\ \ell)$ harmonic diffraction peaks, observed on the diffractogram of Fig. 4.a, correspond to the different crystallographic c parameters of each pure C_n , contained in the mixture of the unmelted powders.

The observation of a single class of $(0\ 0\ \ell)$ diffraction lines on the diffractogram of sample No 1 (Fig. 4b) points to the existence of:

- a single molecule layer stacking periodicity along the long c -axis and consequently,
- a single multi- C_n solid phase.

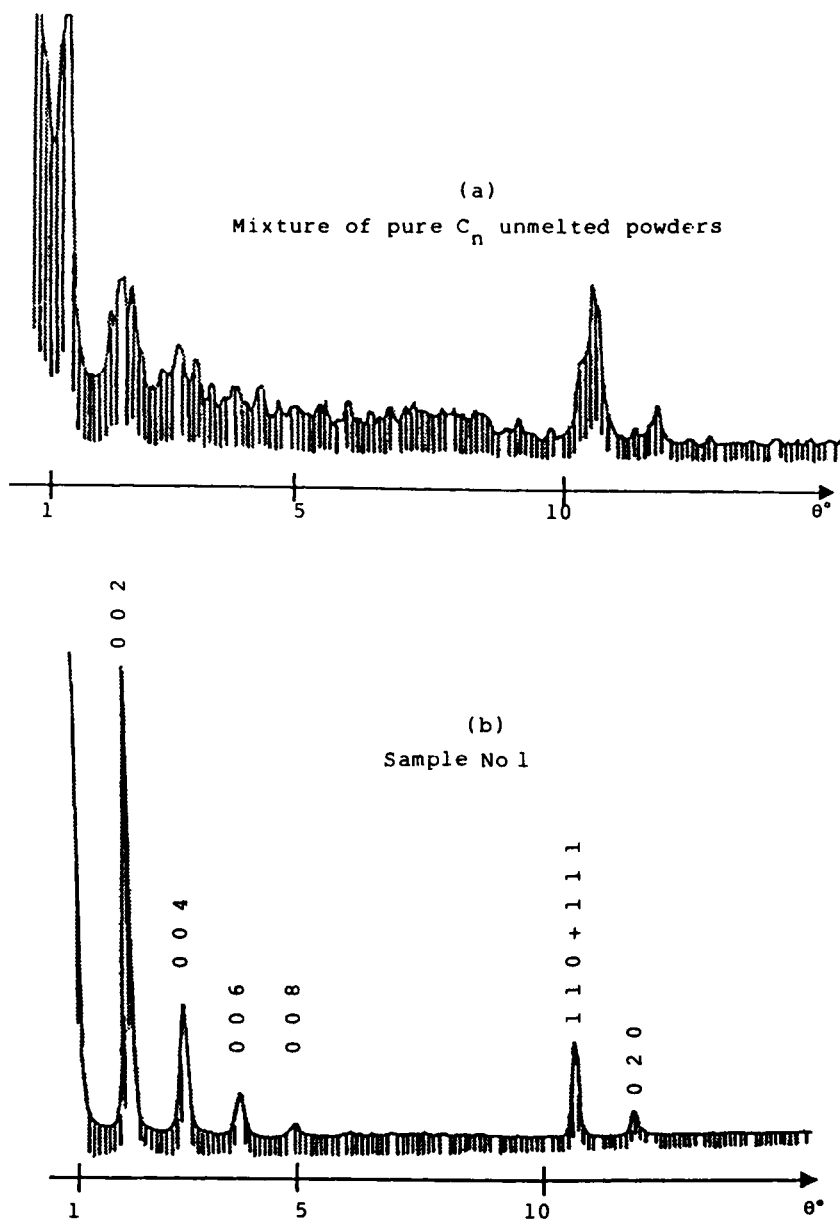


FIGURE 4 Diffraction-X scattering patterns (θ° - λ Cu K_α) of a mixture of the unmelted powders of nine pure C_n ($28 \leq n \leq 36$) (a) and of sample No 1 (b): the diffractogram (a) presents all the series of $(0\ 0\ \ell)$ harmonic lines, corresponding to each pure C_n separately; a single family of $(0\ 0\ \ell)$ harmonic peaks is observed on the pattern (b) of multi- C_n sample No 1, which consists of 23 C_n ($20 \leq n \leq 42$) and which thus forms a single multi- C_n solid solution

The other diffraction peaks are characteristic of an orthorhombic structure, isostructural to the β' intermediate solid solution, observed in binary and ternary mixtures of C_n [5–7]. From the experimental values of the crystallographic c -parameter, determined for each multi- C_n solid solution, it is possible to calculate the \bar{n}_c mean number of carbon atoms per molecule from the relationship established by CHEVALLIER et al. [8] with the literature structural data of pure odd-numbered C_n ($n \leq 41$, Pbcm) [17]:

$$\bar{n}_c = \frac{d - 3.15}{1.27} + 1$$

where $d(\text{\AA})$ is equal to $c(\text{\AA})/2$ and corresponds to the thickness of the molecule layer for the orthorhombic structures of pure C_n ($n \leq 41$, Pbcm) and their molecular alloys.

Table II compares the \bar{n} and \bar{n}_c average numbers of carbon atoms, determined from the chromatographic analyses and from X-ray diffraction respectively. These results show that the multi- C_n mixtures with concentration distributions of the “normal logarithmic” type form a single solid phase whose long crystalline c -axis corresponds to the chain length of a hypothetical pure C_n with \bar{n}_c mean number of carbon atoms almost equal to the \bar{n} average composition in carbon atoms of mixtures: \bar{n}_c always presents an excess value close to 1 in relation to \bar{n} .

TABLE II Comparison between the average carbon atom numbers \bar{n}_c and \bar{n} determined from the c -parameter ($d = c/2$) and by chromatography respectively. The relative uncertainty in the determination of d (\AA) and its corresponding carbon atom number \bar{n}_c values is evaluated at 1.5 %

Sample	$d/\text{\AA}$	\bar{n}_c	\bar{n}	$\Delta n = \bar{n}_c - \bar{n}$
No 1	35.7	26.6	25.5	1.1
No 2	36.8	27.5	26.4	1.1
No 3	38.4	28.7	27.7	1.0
No 4	40.6	30.4	29.4	1.0
Para 1,2	36.1	26.9	26.0	0.9
Para 1,3	37.7	27.4	26.6	0.8
Para 1,4	37.8	28.2	27.2	1.0
Para 2,3	37.5	28.0	27.1	0.9
Para 2,4	38.6	28.8	27.7	1.1
Para 3,4	39.8	29.7	28.5	1.2

Synthetic mixture with a C_n molar concentration distribution of the "decreasing exponential" type

The diffraction-X scattering pattern (Fig. 5) carried out on sample No 5 (C_{18} to C_{36}) at 287.15 K shows in the region of small Bragg angles, three different series of $(0\ 0\ \ell)$ harmonic diffraction peaks (Table III) which indicate the existence of three molecule layer stacking periodicities and thus the presence of three crystal-line multi- C_n solid solutions with three different mean numbers of carbon atoms.

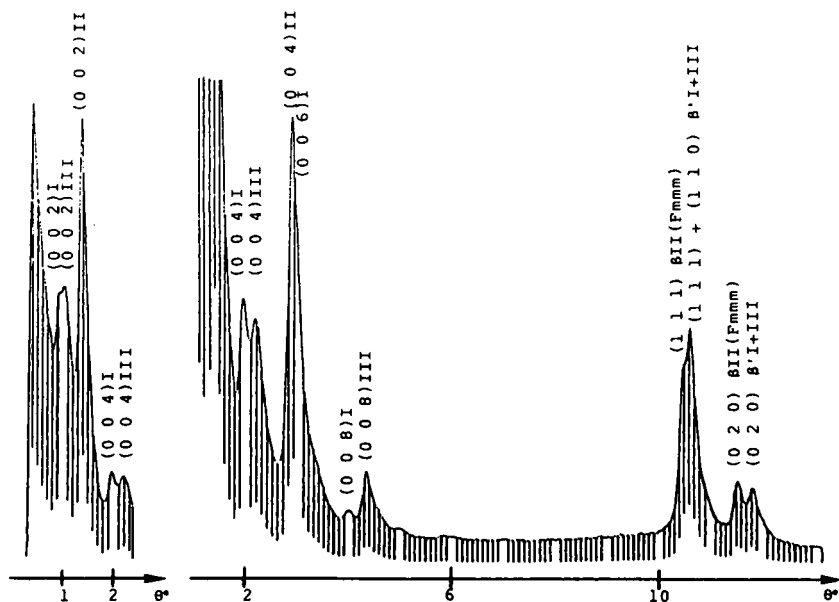


FIGURE 5 Diffraction-X scattering pattern (θ° - λ Cu $K\alpha$, $T = 287.15$ K) of synthetic sample No 5 whose C_n molar concentrations present a distribution of the "decreasing exponential" type: observation of three series of $(0\ 0\ \ell)$ harmonic Bragg-peaks, corresponding to three different molecule layer thickness of three multi- C_n solid solutions. The splitting of the $(0\ 2\ 0)$ diffraction line highlights the presences of the β (Fmmm) disordered phase in RI-Rotator state and of the β'_I and β'_{III} ordered intermediate phases

The other diffraction lines are characteristic of orthorhombic structures and the splitting of the $(0\ 2\ 0)$ diffraction peak highlights the existence of the β (Fmmm) disordered phase and the β' ordered intermediate phase.

The $d(\text{\AA})$ values of the molecule layer thickness of each multi- C_n solid solution and the corresponding average number of carbon atoms of solid phases are reported in Table III as a function of the temperature. From these observations it appears that sample No 5, whose C_n molar concentrations show a distribution of

the "decreasing exponential" type, consists of three different multi- C_n solid phases at 287.15 K:

- i) the two heavier in carbon atoms are isostructural to the β' ordered intermediate phase, denoted β'_I and β'_{III} , with carbon atom mean numbers equal to 31.6 ± 0.5 and 27.7 ± 0.4 respectively.
- ii) the third solid solution, whose average number of carbon atoms is equal to 20.8 ± 0.3 , presents the structure of the β (Fmmm) disordered phase: it is called β_{II} (Fmmm).

TABLE III Variations of the $d(\text{\AA})$ molecule layer thickness and the corresponding \bar{n}_c mean number of carbon atoms and evolutions of the phases versus the decreasing temperature in the course of the crystallization of synthetic sample No 5 ($C_{18} - C_{36}$). The relative uncertainty in $d(\text{\AA})$ and \bar{n}_c determination is evaluated at 1.5 %

Temperature	first solid solution I			second solid solution II			third solid solution III		
	$d/\text{\AA}$	\bar{n}_{cI}	phase	$d/\text{\AA}$	\bar{n}_{cII}	phase	$d/\text{\AA}$	\bar{n}_{cIII}	phase
326.15	←					liquid			→
324.15	44.5	32.5	↑			+	liquid		
320.15	43.6	31.8							
318.15	43.6	31.8		38	27.4	↑			
315.15	43.6	31.8		36.5	26.2				
313.15	43.3	31.6		35	25		+	liquid	
311.15	43.5	31.7		33.9	24.1	$\alpha_{II}\text{-RII}$			
308.15	43.3	31.6		32.8	23.3		solid state		
305.15	43.6	31.8		31.8	22.5	↓			
304.15	43.3	31.6		31.7	22.4	↑			
301.15	43.4	31.6		30.9	21.8		41.3	30	↑
298.15	43.5	31.7		30.8	21.7		41.3	30	
295.15	43.5	31.7	β'_I	30.8	21.7		40	28.9	
294.15	43.4	31.6		30.3	21.3		40	28.9	
292.15	43.5	31.7		30.3	21.3		39.4	28.5	
290.65	43.4	31.6		30	21.1	$\beta_{II}\text{-RI}$	38.7	27.9	
288.15	43.6	31.8		30	21.1		38.7	27.9	
287.15	43.4	31.6		29.6	20.8		38.7	27.7	β'_{III}
286.15	43.6	31.8		29.7	20.9		38.5	27.8	
284.65	43.6	31.8		29.4	20.6		36.4	26.1	
283.15	43.3	31.6		29.4	20.6		36.4	26.1	
280.15	43.3	31.6		28.8	20.2	↓	36.4	26.1	
275.15	43.3	31.6	↓	28.6	20	β'_{II}	36.4	26.1	↓

Differential thermal analyses (DTA) were performed using a SETARAM Differential Scanning Calorimeter (DSC III) of the Tian Calvet type. Multi- C_n sample No 5, preliminarily melted and slowly cooled in the measuring crucible, was heated from 253.15 K to 333.15 K at a rate of 0.5 K.min⁻¹ and cooled in the same temperature range at the same rate (Fig. 6).

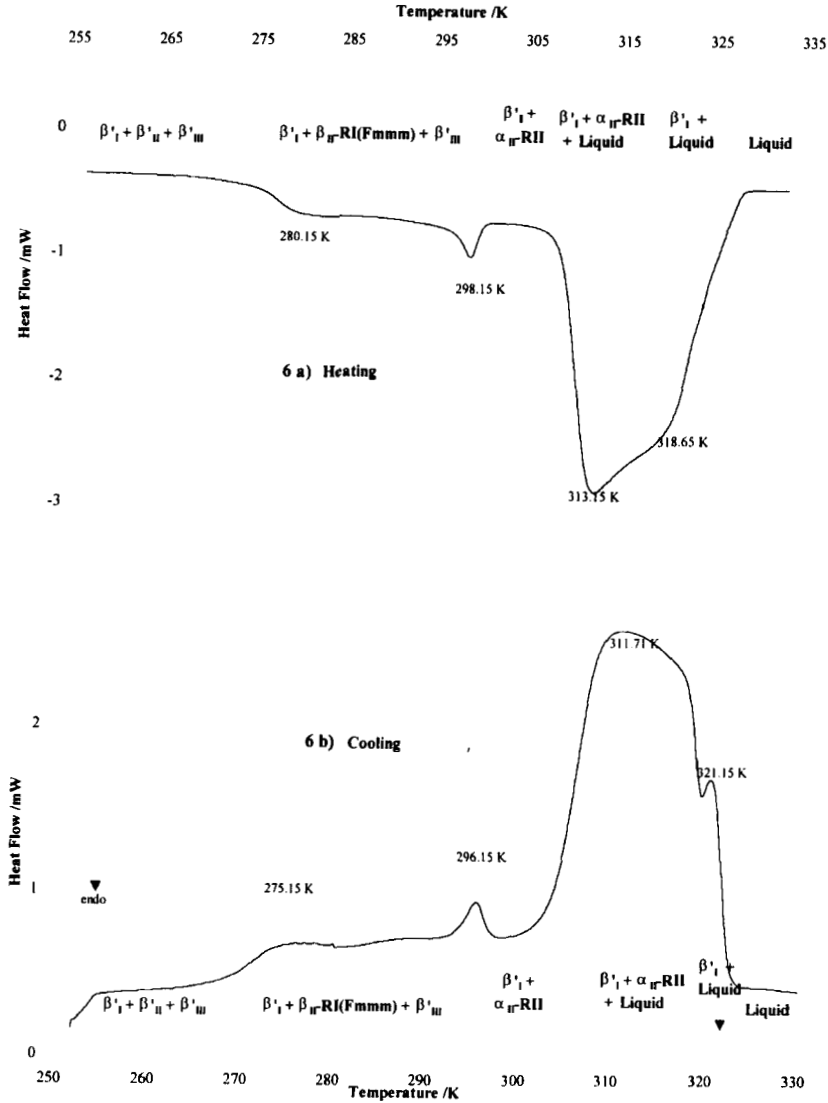


FIGURE 6 Thermogram carried out by differential scanning calorimetry in the course of heating (a) and cooling (b) (0.5 K.mn⁻¹) from 255.15 K to 330.15 K and vice versa

Four thermal effects were observed in the course of the heating and cooling; they were characterized by the peak top temperatures (Fig. 6), which present a hysteresis phenomenon during the cooling. In view of the complexity of thermograms, X-ray diffraction experiments were carried out at different temperature levels from the liquid state to 275.15 K (rate of cooling = 1 K.mn^{-1} , length of each isothermal level = one hour); the results appear on Fig. 7 and in Table III and lead to the following observations when the temperature decreases from liquid state:

i) First, a single series of $(00\ell)_I$ small Bragg angle diffraction peaks appears on the X-ray diffractograms, recorded just below the crystallization onset temperature (Fig. 7 a) and at 320.15 K: this observation shows that the first deposits form a single solid solution I; moreover in this temperature range, the \bar{n}_{cI} mean number of carbon atoms, determined from X-ray long spacings (Table III), varies from 32.5 ± 0.5 to 31.8 ± 0.5 ; these values are smaller than 36, corresponding to the carbon atom number of the longer chain of the mixture and indicate that lighter alkanes are already present in solid deposit just below the crystallization onset temperature as determined by chromatography analyses of C_n concentrations of first solid deposits in the course of the crystallization of the same multi- C_n mixture in C_{10} [15]. The diffusion halo (Fig. 7a) corresponds to the liquid phase.

The crystallization onset of the first β'_I multi- C_n solid solution I was characterized on the D.T.A. thermogram (Fig. 6b) by the thermal effect whose top temperature was equal to 321.15 K in the course of cooling:

ii) Then, a second class of $(00\ell)_{II}$ harmonic lines of X-ray diffraction (Fig. 7 b-b') occurs from 318.15 K to 304.15 K, corresponding to a second solid solution II. In this temperature interval, the \bar{n}_{cI} average number of carbon atoms of the first solid solution I is unchanging and equal to almost 31.7 ± 0.5 (Table III); that of the second solid solution II, \bar{n}_{cII} , varies from 27.4 to 22.4 (± 0.3).

When the temperature decreases the intensity of the diffusion halo corresponding to the liquid phase decreases and it seems that the halo disappears at 310.15 K. The thermal peak, whose top temperature was equal to 311.71 K (Fig. 6 b), was caused by the crystallization of this second multi- C_n solid solution II.

iii) Finally, a third series of $(00\ell)_{III}$ diffraction peaks is observed at 301.15 K (Fig. 7c-d), it characterizes the third solid solution III. In the temperature range from 301.15 K to 275.15 K, the \bar{n}_c average numbers of carbon atoms behave as follows (Table III):

- for the solid solution I, \bar{n}_{cI} , unchanging and equal to almost $31.7 (\pm 0.5)$

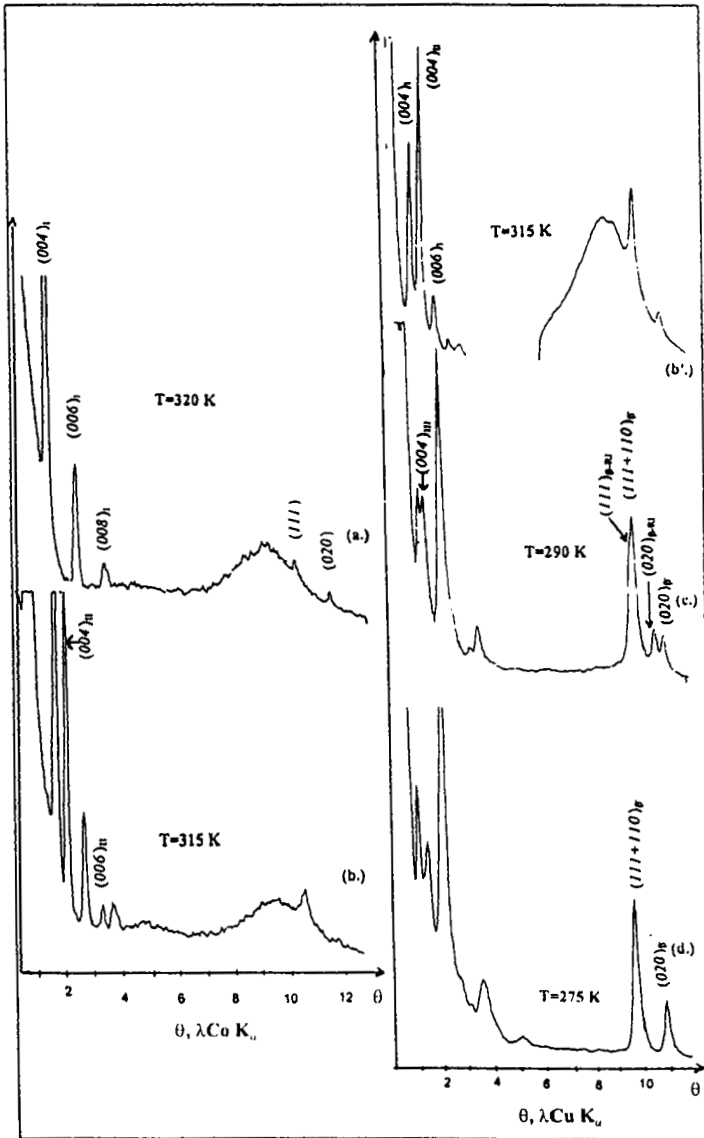


FIGURE 7 Structural evolutions in the course of the crystallization of synthetic sample No 5 whose C_n molar concentration distribution presents the "decreasing exponential" type from C_{18} to C_{36} : a single series of $(00\ell)_I$ lines is observed on pattern (a) (θ° - λ Co K_α); a second series appears on the diffractograms b- $(\theta^\circ$ - λ Co K_α) - b'-(θ° - λ Cu K_α) and a third on the patterns c-d (θ° - λ Cu K_α). The diffusion halo corresponds to the liquid phase: its intensity decreases in the course of the crystallization of the different multi- C_n solid solutions; it seems that it disappears at a temperature close to 310.15 K before the appearance of the third β'_{III} solid solution III

- for the solid solution II, \bar{n}_{cII} , varying from 21.8 to 20 (± 0.3)
- and from 30 to 26.1 (± 0.4) for \bar{n}_{cIII} of the solid solution III.

The thermal effect with the top temperature equal to 296.15 K (Fig. 6 b) characterized the appearance of the third multi- C_n solid solution III.

The other diffraction peaks are characteristic of orthorhombic structures and correspond to the β' ordered intermediate phase for the solid solutions I and III. For the solid solution II, the splitting of the (0 2 0) diffraction peaks (Fig. 7 c) indicates the existence of the β (Fmmm) disordered phase in Rotator I state into the temperature range from 304.15 K to 283.15 K.:

i) above 304.15 K the observation of a (0 2 0) single diffraction line (Fig. 7 b-b'), characteristic of the presence of the β' ordered phase, indicated that the multi- C_n solid solution II underwent the transition $\beta_{II}\text{-RI(Fmmm)} \rightarrow \alpha_{II}\text{-RII(R}\bar{3}\text{m)}$.

ii) between 280.15 K and 275.15 K, the disappearance of the splitting of the (0 2 0) diffraction peaks (Fig. 7d) corresponded to the disordered \leftrightarrow ordered transition $\beta_{II}\text{(Fmmm)} \leftrightarrow \beta'_{II}$ of this multi- C_n solid solution II which was highlighted by the thermal effect whose top temperature is equal to 275.15 K in the course of cooling and 280.15 K in the course of heating (Fig. 6) (Table III).

CONCLUSION

Commercial samples No 1, 2, 3 and 4 and their fifty-fifty weight percent mixtures, which present C_n molar concentration distributions of the "normal logarithmic" type, form a single multi- C_n solid solution isostructural to the β' ordered intermediate phase of binary and ternary C_n alloys [5–7]; the periodicity of the molecule layer stacking corresponds to that of a hypothetical pure C_n whose \bar{n}_c mean number of carbon atoms is equal to the \bar{n} average number of carbon atoms of the multi- C_n mixture with an excess value close to one carbon atom. In these kinds of mixtures, the crystalline structure and the corresponding molecule layer thickness of the single multi- C_n solid solution is imposed by the C_n whose chain lengths have numbers of carbon atoms close to the \bar{n} mean number of carbon atoms of the molar concentration distribution and which are in the majority.

Synthetic sample No 5 which consists of a C_n molar concentration distribution of the "decreasing exponential" type from C_{18} to C_{36} presents at 287.15 K three multi- C_n solid solutions; the \bar{n}_c average numbers of carbon atoms per molecule, determined from the three periodicities of molecule layer stacking, are equal to 31.6 ± 0.5 , 27.7 ± 0.4 and 20.8 ± 0.3 respectively:

- the two heavier solid solutions I and III (β'_I and β'_{III}) have the structure of the β' ordered intermediate phase of the C_n binary alloys.
- the lighter II presents the β -(Fmmm) disordered phase in the RI Rotator state.

With decreasing temperatures from the liquid state these three solid phases appear successively as follows: first the β'_I multi- C_n solid solution I with a \bar{n}_{cI} mean number of carbon atoms equal to 32.5 ± 0.5 then the β_{II} (Fmmm) solid solution II in the RI-Rotator state whose \bar{n}_{cII} average number of carbon atoms is equal to 27.4 ± 0.4 , finally the third β'_{III} solid solution III with a \bar{n}_{cIII} equal to 30 ± 0.5 ; as the temperature decreases, these average numbers of carbon atoms decreases as the ratio of smaller alkanes gradually increases in the three multi- C_n solid solutions (Table III). The (β'_I and β'_{III}) multi- C_n solid solutions I and III always are isostructural to the β' C_n binary intermediate solid solution whereas the multi- C_n solid solution II successively presents the α_{II} ($R\bar{3}m$) phase in RII-Rotator state, then the β_{II} (Fmmm) disordered phase in the RI-Rotator state, finally the β'_{II} ordered phase. At the solid state, this type of sample No 5 is made up of three phases; because in the C_n molar concentration distribution of the “decreasing exponential” type, the smaller chains, which here are in the majority, do not succeed in making the longer chains bend, which are too numerous, to form a single solid solution, as also observed by infrared and Raman spectroscopies by CLAVELL-GRUNBAUM *et al.* [18]

Acknowledgements

We are indebted to Mr Geoffrey SOCKETT, Professor of English at Ecole Nationale Supérieure des Industries Chimiques, for the correction of this manuscript and to Mr Luc BENOIST, application Manager at SETARAM Company, for the experiment of differential thermal analyses.

References

- (1) J.J. Retief and J.H. Le Roux, *South Africa J. of Sc.*, **79**, 234, (1983).
- (2) S.R. Craig, G.P. Hastie, K.J. Roberts, A.R. Gerson, J.N. Sherwood, R.D. Tack, *J. Mater. Chem.*, **8**, 859, (1998).
- (3) M. Dirand, V. Chevallier, E. Provost, M. Bouroukba, D. Petitjean, *Fuel*, **77**, 1253, (1998).
- (4) V. Chevallier, E. Provost, J.B. Bourdet, M. Bouroukba, D. Petitjean, M. Dirand, *Polymer*, **40**, 2121, (1999).
- (5) M. Dirand, Z. Achour, B. Jouti, A. Sabour, J.C. Gachon, *Mol. Cryst. Liq. Cryst.*, **275**, 293, (1996).
- (6) H. Nouar, D. Petitjean, M. Bouroukba and M. Dirand, *Mol. Cryst. Liq. Cryst.*, **309**, 273, (1998).
- (7) H. Nouar, D. Petitjean, M. Bouroukba and M. Dirand, *Mol. Cryst. Liq. Cryst.*, **326**, 381, (1999).
- (8) V. Chevallier, D. Petitjean, V. Ruffier-Meray, M. Dirand, *Polymer*, **40**, 5953, (1999).
- (9) A. Muller, *Proc. Roy. Soc.*, **A 127**, 514, (1930).
- (10) G. Ungar, *J. Phys. Chem.*, **87**, 689, (1983).
- (11) J. Doucet, I. Denicolo, A.F. Craevich, G. Germain, *J. Chem. Phys.*, **80**(4), 1647, (1984).
- (12) G. Ungar, G.J. Masic, *J. Phys. Chem.*, **89**, 1036, (1985).
- (13) J.L. Daridon, P. Xans, F. Montel, *Fluid Phase Equilibria*, **241**, (1996).

- (14) J. Pauly, C. Dauphin, J.L. Daridon, *Fluid Phase Equilibria*, **149**, 14, 191, (1998).
- (15) C. Dauphin, J.L. Daridon, J. Coutinho, P. Baylere, M. Potin-Gautier, *Fluid Phase Equilibria*, **161**, 135, (1999).
- (16) J. Didelon, J.P. Emeraux, G. Bodez, C. Gleitzer, *Rev. Phys. Appliquée*, **14**, 541, (1979).
- (17) S.R. Craig, G.P. Hastie, K.J. Roberts and J.N. Sherwood, *J. Mater. Chem.* **4**, 977, (1994).
- (18) D. Clavell-Grunbaum, H.L. Strauss, R.G. Snyder, *J. Phys. Chem.* **B 101**, 335, (1997).